Assessment of Retrieved GMI Emissivity Over Land, Snow, and Sea Ice in the GEOS System

Bryan M. Karpowicz[1,2,3], Yanqiu Zhu[1], and S. Joseph Munchak[4]

1. NASA Global Modeling and Assimilation Office (GMAO)
2. Goddard Earth Sciences Technology and Research (GESTAR)
3. Universities Space Research Association
4. Mesospheric Atmospheric Processes Laboratory

GMAO
Global Modeling & Assimilation Office

1. Introduction

Measurements from microwave sounders and imagers provide a valuable source of information including atmospheric temperature and water vapor in Numerical Weather Prediction (NWP) systems that assimilate these observations directly over water surfaces (oceans and other large water bodies). In a recent decadal survey, targeted observables in the Planetary Boundary Layer (PBL) were cited as a key need for future observations (NASEM, 2018). Microwave observations which sense in the PBL are currently available, however, utilizing surface-sensitive microwave observations for atmospheric data assimilation remains a challenge over land, snow and sea ice. This is in part due to the inability of surface emissivity models used by NWP data assimilation systems to simulate observations with sufficient accuracy. The GEOS-ADAS (Todling and el Akkraoui, 2018) which utilizes the Community Radiative Transfer Model (CRTM) (Han, 2006; Chen 2009) is no exception. The ECMWF system has retrieved instantaneous surface emissivity from surface-sensitive channels for SSMI/S and MHS radiance observations, and apply these estimates to the closest channels higher in frequency (Baordo and Geer 2016) in the calculation of simulated radiances. This approach currently is also being tested in the GEOS-ADAS for AMSU-A and ATMS radiances (Zhu et al. 2021). No or minimal emissivity spectral variability has been assumed in the above-mentioned studies. Recently, work by Munchak et al., 2020 (hereby referred to as M2020) provided a new database for emissivity over land, snow and sea ice retrieved from the NASA Global Precipitation Mission (GPM). Compared with Tool to Estimate Land Surface Emissivities at Microwave (TELSEM[2]; Wang et al., 2017), M2020 provides emissivities for more frequencies (i.e., 10.7 GHz V/H). Moreover, this database is unique in that it utilizes both active and passive data to retrieve surface emissivity and normalized radar cross section. While the emissivity values may be useful for other sensors, they are most applicable to the GPM Microwave Imager (GMI). In this work the GEOS-ADAS is modified to utilize emissivity values from Munchak et al, 2020 in place of values used by CRTM. Presently, only GMI radiances over ocean are used in the operational GEOS-ADAS. This study will focus on the GMI radiances over land, snow, and ice, as a first attempt to evaluate GMI radiances over these non-water surface types. Two cases are then presented, one with one week of observation minus background departures using the modified GEOS-ADAS, and one utilizing the original GEOS-ADAS. It should be noted that the surface emissivity models in CRTM are not state of the art and are scheduled to be replaced by the Community Surface Emissivity Module (CSEM; Chen and Weng, 2016). Simulations using default CRTM emissivity values are used merely as reference comparing against M2020, and is not a thorough comparison against other more state of the art modules such as CSEM.

2 Microwave Emissivity Surface Databases and Models

2.1 Emissivity available in CRTM

The control case in this work utilizes the default emissivity models over land, snow, and sea ice available for GMI in the CRTM. As mentioned previously, the emissivity models utilized by the CRTM are sensor specific, however, in the case of GMI there are no derived empirical or semi-empirical models for snow or sea ice. The LandEm physical model provides emissivity values for frequencies below 80 GHz over land and snow-covered surfaces. LandEm is a physical model derived from a 3-layer radiative transfer model along with modified Fresnel equations at layer interfaces. The model uses several parameterizations, and variables obtained from the GEOS system such as Leaf Area Index (LAI), snow depth, surface type, along with sensor view geometry parameters such as zenith angle. It was validated with available data at the time from ground-based measurements (Mätzler, 1994), and satellite data from AMSU-A. For frequencies above 80 GHz, the CRTM will use a constant value of 0.95 for land, and 0.9 for snow. Given there is no empirical model for sea ice available in the case of GMI, the CRTM will use a default value of 0.92. For convenience, the source of emissivity values for each GMI channel are summarized in Table 1.

Table 1: The source of emissivity used by the CRTM for each surface type and GMI Channel

Surface	10.6 GHz V	10.6 GHz H	18.7 GHz V	18.7 GHz H	23 GHz V	37 GHz V	37 GHz H	89 GHz V	89 GHz H	166 GHz V	166 GHz H	183 V +/- 3 GHz	183 V +/- 7 GHz
Land	LandEm	LandEm	LandEm	LandEm	LandEm	LandEm	LandEm	0.95	0.95	0.95	0.95	0.95	0.95
Snow	LandEm	LandEm	LandEm	LandEm	LandEm	LandEm	LandEm	0.9	0.9	0.9	0.9	0.9	0.9
Ice	0.92	0.92	0.92	0.92	0.92	0.92	0.92	0.92	0.92	0.92	0.92	0.92	0.92

2.2 GPM Microwave Imager

Data from the GPM Microwave Imager (GMI) is utilized both in M2020 and in this study. GMI is a 13 channel conically scanning microwave radiometer aboard the Global Precipitation Mission (GPM). Launched in February 2014, GPM is in a non-sun synchronous orbit with an inclination angle of 65°. The conical scan has a nominal Earth incidence angle of 52.8° for channels at or below 89 GHz and 49.2° for channels at or above 166 GHz (Skofronick-Jackson et al., 2017; Petty and Bennartz, 2017). The conical scan geometry with a near constant Earth incidence angle/zenith viewing makes it possible for more accurate emissivity databases specifically designed for GMI as in M2020, given there is an Earth incidence angle dependence on emissivity. The channels for GMI are shown in Table 1, and range in frequency between 10.6-183 GHz. All 13 channels are sensitive to precipitation. The lower frequency channels (10.6-37 GHz) are most sensitive to liquid precipitation, and higher frequencies (89-183GHz) are most sensitive to ice scattering. Channels 12 (183 +/- 3 GHz V), and 13 (183 +/-7 GHz V) are strongly sensitive to water vapor and have a relatively weak surface sensitivity outside polar regions and where ice sheets are present. Channel 5 (23 GHz) along with Channels 10-11 (166 GHz V/H) also have sensitivity to water vapor in addition to surface sensitivity, however, this sensitivity is weaker than the 183 GHz channels. Channels 10-11 are typically considered surface sensitive when column water vapor is approximately less than 20 mm (Munchak et al., 2020). Currently, in the GEOS-ADAS channels are only assimilated over water using 23 GHz, 37 GHz V, 166 GHz V, 183+/-3 GHz V, and 183+/-7 GHz V (Kim et al., 2020). In future assimilation work over land snow and ice, a different channel selection may be necessary. Any remaining emissivity uncertainty may result in large uncertainty in brightness temperature simulation, which may conflate signals from different geophysical parameters.

2.3 Emissivity from Active-Passive Microwave Land Surface Database

Recently, Munchak et al., 2020 presented an Active-Passive Microwave Land Surface Database that includes monthly average emissivity values for GMI Channels 1-11. The average emissivities were derived using 5 years of emissivity retrievals (March 2014-February 2019) using data from GPM, thus providing a climatological emissivity value on a monthly basis. The data is provided using a 0.25x0.25 degree global (67S-67N) grid, with an average value of emissivity at each grid cell over land, snow, and ice (with a fill value for no retrieval). The dataset is unique in that it utilizes the DPR on GMI to both filter out precipitation-contaminated observations, along with retrieval diagnostics and ancillary data from MERRA-2 (Gelaro et al., 2017). The dataset also contains a surface classification based on the spectral emissivity and radar backscatter cross-section characteristics. The retrieval of emissivity uses GMI brightness temperatures taken from the Level -1CR data product, surface normalized radar cross section (σ_0) from the DPR Level 2A data product, along with data from MERRA-2 which is used as the a-priori atmospheric profiles and surface temperature for the retrieval of emissivity from brightness temperatures.

Figure 1 shows observations simulated and compared in this study. It should be noted that there are no retrieved 166 GHz emissivities over portions of Africa and South America in the M2020 dataset due to insufficient sensitivity of this channel to the surface in these regions due to high water vapor amounts, To simplify the implementation, no observations considered over these regions (in white).

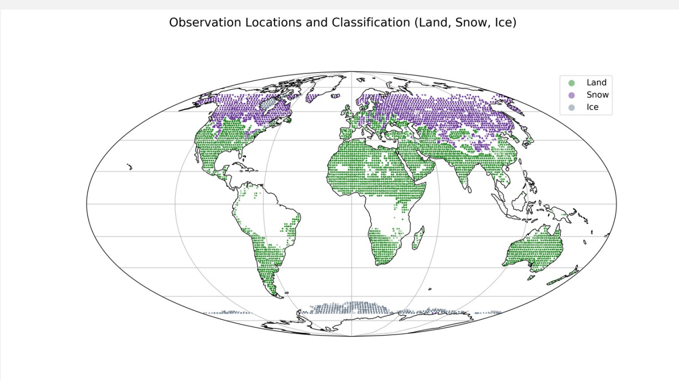

Figure 1: Locations of all GMI observations over Land, Snow and Ice used in this study

3. Evaluation of Active-Passive Microwave Surface Database using GEOS

In this work the emissivity models available in the GEOS-ADAS are compared against those available in M2020. GMI has 13 channels, with varied sensitivity to the surface. the two water vapor channels at 183 GHz having less surface sensitivity than others outside polar regions, or regions with ice sheets . Currently, the GEOS-ADAS only assimilates 23 GHz, 37 GHz V, 166 GHz V, and two vertically polarized water vapor channels at 183 GHz over ocean. No GMI radiances over land, snow and ice are used. This resulted in some slight modifications to the GEOS-ADAS along with some other quality control decisions. These are described in Section 3.1, and in Section 3.2 observations using the default GEOS-ADAS emissivity models are compared against that of M2020.

3.1 Evaluation method using the GEOS-ADAS

The comparisons made in this study use two slightly modified versions of the GEOS-ADAS version 5.27.1. Most of the code changes are common among both systems. First, version 5.27.1 of the GEOS-ADAS rejects observations over land, snow, ice and mixed surfaces. This check is modified to only reject mixed surfaces for both cases. While having the ability to simulate mixed surfaces is desirable, as a first step to evaluate the emissivity database of M2020, it is best to compare surfaces without the complexity of accounting for surface cover fractions which may introduce more representativeness error. Next, a quality control check that rejects observations north of 55 degrees latitude, and south of -55 degrees latitude is removed. This check was originally added to the GEOS-ADAS to avoid sea ice. A goal of this study is to investigate the ice emissivity available in M2020 and compare it to the default values in CRTM for comparison, therefore, the latitude check is removed for both simulations. Finally, to avoid the complexities of comparing regions affected by rain or clouds a check is added to flag observations with a total sum of ice and liquid water content of 0.15 kg/m^2 and remove them from consideration.

For the case using M2020 there were a few steps necessary to ingest emissivity into the GEOS-ADAS. First, a netcdf file was generated based on data provided in M2020. The emissivity dataset is a 5-dimensional array indexed by channel, latitude, longitude, month, and surface type (land, snow, or sea ice). Each observation is interpolated using a nearest neighbor approach to the M2020 latitude and longitude grid . The month of the observation is used as an index along with the surface type given by the GEOS-ADAS. For the two 183 GHz channels, there are no retrieved values available from M2020. Instead, the emissivity values from the 166 GHz V channel are used to approximate the emissivity value. A similar assumption was made in Baordo and Geer 2016, using 89 GHz emissivity values to estimate 183 GHz emissivity for the SSMIS instrument. The use of 166 GHz V is closer in frequency and may provide a better estimate of emissivity.

Radiative transfer calculations are performed by running the GSI in a standalone mode in place of a full 4D-EnVar experiment. In standalone mode, the background fields are taken from an existing baseline run. This allows a quick method to produce simulated observations for comparison of the emissivity models, and since the background fields are constant in the comparisons, the only differences are due to the changes in emissivity in the radiative transfer calculations. The background fields are on hourly intervals and are interpolated in space and time to the observation location. One week of observations are simulated for December 1, 2020 through December 7, 2020. In all comparisons to follow the observation minus background values are used to indicate whether the emissivity model improves the simulation. A smaller magnitude (absolute value) observation minus background indicates the simulation is closer, and therefore considered an improvement. In all comparisons, no bias correction is applied to the simulated values.

3.2 Results of Evaluation

The simulated brightness temperatures (also commonly referred to as the background) using M2020 and using the default CRTM are compared against GMI observations for the first week of December 2020. In Figure 2, scatter plots observation minus background (OMB) are shown for the 13 GMI channels. One feature that clearly stands out is ice (in orange) and snow surfaces (in blue) exhibit the largest scatter in OMB values in both in the M2020 simulation and default CRTM simulation relative to Land (in green). Next, departures over land are significantly smaller for M2020 in panels A-G. It is also shown that the large OMBs over ice of horizontal polarization channels (panels B, D, G, I) using the default CRTM are significantly improved by using M2020. Finally, it is clear the default CRTM exhibits a bias over ice in panels A-I and over snow in panels H-M (values not centered around zero), whereas in the M2020 simulation the values are closely centered around zero. For reference, all observation points and their classification as either over land, snow are ice are shown in Figure 1.

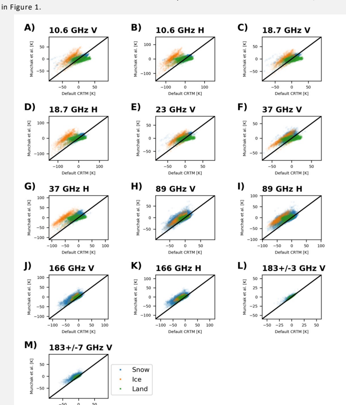

Figure 2: Scatter plots of GEOS-ADAS calculated values of observation minus background using Munchak et al., 2020 vs default CRTM values.

Next, OMB values are averaged spatially on a 2.5 x 2.5 degree averaging grid over the week and plotted spatially, while all observation locations are used to compute histograms in Figures 3 and 4. In each panel, the 2D map plot in the upper part shows the averaged OMB at each gridbox, and the plot in the lower part displays histograms for all data (shaded area), data over land (green line with squares), over ice (gray line with triangle), and over snow (purple line with circle), respectively. Significant improvements can be observed in Figure 4 (M2020 simulation) vs Figure 3 (CRTM default) spatially. First, there are far fewer points in yellow indicating outside the +/- 10 K range. Next, there are many more regions that are in the +/- 5K OMB range in Figure 4 vs Figure 3. Moreover, when CRTM default emissivities are used, the OmB values of the channels with horizontal polarization are much worse than those vertical polarization; but when M2020 emissivities are used, the OmB differences between horizontal and vertical polarization are decreased. These results are in agreement with those observed in Figure 2.

Observing the histograms of OMB values in Figures 3-4, in Figure 4 there is a clear gaussian pattern nearly centered around zero for all channels. Figure 3 only has a gaussian pattern for frequencies at 89 GHz and above (Panels H-M), with a significant bias for the 89 GHz H polarization channel and a moderate bias for the 166 GHz H polarization (Panels I and K). The two 183 GHz channels have little sensitivity to surface, especially the +/- 3 GHz channel which has a sensitivity which peaks higher in the atmosphere. The improvements are further shown in Figure 5 which contains spatial plots and histograms of the difference between the absolute values of OMB simulations using M2020 minus the absolute values of OMB using the default CRTM. Negative values indicate the M2020 simulation is closer (blue), positive values (red) indicate it is further away. Overall, with exception to the 183 GHz +/-3 channel (Panel L), there are many points where the OMB simulated using M2020 is closer.

Next, the relative improvement over land, snow, and ice are considered. Comparing both spatially and viewing histograms in Figures 1, 3 and 4, there are clear improvements over land. Comparing the histograms over land (green squares), there is a clear gaussian pattern with a nearly centered around zero for all channels for M2020 (Figure 4), whereas in Figure 3 there are cases where there is a gaussian pattern for the default CRTM case, however, for all channels there is an improvement for the M2020 case (Figure 4). For points identified as snow covered for the default CRTM and M2020 simulations in Figures 3-4, improvements are still noticeable, they are far less dramatic with long tails remaining in the distribution for Figure 4. Comparing histograms and spatial distributions of OMB over ice in Figures 3-4, there are improvements, however, the improvements are not as dramatic as either over land or snow.

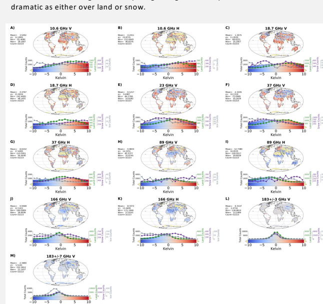

Figure 3: GEOS-ADAS calculated values of observation minus background using default CRTM values.

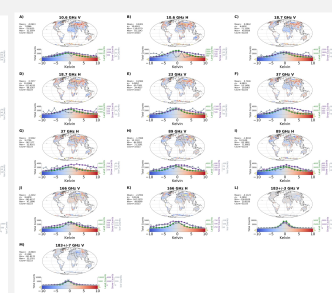

Figure 4: GEOS-ADAS calculated values of observation minus background using Munchak et al., 2020.

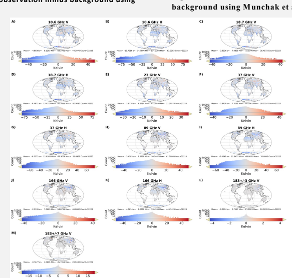

Figure 5: Difference in GEOS-ADAS calculated absolute values of observation minus background using Munchak et al., 2020 minus values calculated with default CRTM.

4. Summary

In this work it has been shown that using emissivity values from M2020 can improve simulation of brightness temperatures from GMI using the GEOS-ADAS. The improvements are most noticeable over land with a dramatic improvement, followed by snow and ice with a less dramatic improvement. With such a dramatic improvement over land, it may be possible to attempt assimilating surface sensitive GMI channels over land, or at the very least as a first guess for an in-line retrieval or adding emissivity to the GEOS-ADAS control vector. Assimilating surface sensitive channels over land could provide information regarding temperature and moisture in the Planetary Boundary Layer in the GEOS-ADAS. This was noted as a key need by the decadal survey (NASEM, 2018), and is an on-going effort at the Global Modeling and Assimilation Office. Additionally, it may be possible to utilize M2020 for similar sensors such as AMSR-2 which has an Earth incidence angle of 55° (Maeda et al., 2016), however, this would require rigorous testing. Full observing system experiments will be conducted using surface sensitive channels over land, snow and sea ice which could provide more data in the planetary boundary layer, thus improving its representation in the GEOS system.

Acknowldegements

We would like to thank the NASA GSFC Science Task Group (STG) on "Evaluation and Improvement of Surface Emissivity for Enhanced Earth and Planetary Remote Sensing" for support, and funding to conduct this study.

References

Aires, F., Prigent, C., Bernardo, F., Jiménez, C., Saunders, R., Pascal, B.: A Tool to Estimate Land-Surface Emissivities at Microwave frequencies (TELSEM) for use in numerical weather prediction, *Quarterly Journal of the Royal Meteorological Society*, 137(656), pp. 690–699, doi: 10.1002/qj.803, 2011.

Baordo, F and Geer A.: Assmilation of SSMIS humidity-sounding channels in all-sky conditions over land using a dynamic emissivity retrieval, *Quarterly Journal of the Royal Meteorological Society*, 142, pp. 2854–2866, doi: 10.1002/qj2873, 2016.

Chen, M. and Weng, F.: Modeling land surface roughness effect on soil microwave emission in community surface emissivity model, IEEE Transactions on Geoscience and Remote Sensing. IEEE, 54(3), pp. 1716–1726, doi: 10.1109/TGRS.2015.2487885, 2016.

Chen, Y., Weng, F., Han, Y. and Liu, Q.: Validation of the community radiative transfer model by using CloudSat data. Journal of Geophysical Research Atmospheres, 114, 1–15,doi: 10.1029/2007JD0095612009, 2009.

Han, Y., van Delst, P., Liu, Q.,Weng, F., Yan, B., Treadon, R. and Derber, J.: NOAA Technical Report NESDIS 122 JCSDA Community Radiative Transfer Model (CRTM)-Version 1. NOAA Tech Report, 2006.

Gelaro, R. , McCarty, W., Suárez, M.J., Todling, R., Molod, A., Takacs, L., Randles, C. A., Darmenov, A., Bosilovich, M. G., Reichle, R., Wargan, K., Coy, L., Cullather, R. Draper, C., Akella, S., Buchard, V., Conaty, A., da Silva, A.M., Gu, W., Kim, G. K., Koster, R. Lucchesi, R., Merkova, D., Nielsen, J. E., Partyka, G., Pawson, S., Putman, W., Rienecker, M., Schubert, S.D., Sienkiewicz, M., Zhao, B.: The modern-era retrospective analysis for research and applications, version 2 (MERRA-2), Journal of Climate, 30(14), pp. 5419–5454, doi: 10.1175/JCLI-D-16-0758, 2017.

Kim, M., Jin,J., Akkraoui, A.E., McCarty, W., Todling,R., Gu, W., Gelaro, R.:**The framework for assimilating all-sky GPM microwave imager brightness temperature data in the NASA GEOS data assimilation system** Mon. Weather Rev., 148, pp. 2433-2455, doi: 10.1175/MWR-D-19-0100.1, 2020

Mätzler, C.: Passive microwave signatures of landscapes in winter, Meteorology Atmospheric Physics, 54, 241-260, doi: 10.1007/BF01030063, 1994.

Maeda,T., Taniguchi, Y., and Imaoka, K. : GCOM-W1 AMSR2 Level 1R Product: Dataset of Brightness Temperature Modified Using the Antenna Pattern Matching Technique, *IEEE Transactions on Geoscience and Remote Sensing*, vol. 54, no. 2, pp. 770-782 doi: 10.1109/TGRS.2015.2465170, 2016.

Munchak, Stephen Joseph, Ringerud, S., Brucker, L., You, Y., de Gelis, I., and Prigent, C.: An Active–Passive Microwave Land Surface Database From GPM, IEEE Transactions on Geoscience and Remote Sensing, Vol 58, Number 9 6224–6242, doi:10.1109/TGRS.2020.2975477, 2020.

National Academies of Sciences Engineering and Medicine (NASEM): Thriving on Our Changing Planet: A Decadal Strategy for Earth Observation from Space. The National Academies Press. Washington, DC, doi: 10.17226/24938, 2018.

Petty, G.W.,Bennartz, R.: Field-of-view characteristics and resolution matching for the Global Precipitation Measurement (GPM) Microwave Imager (GMI), Atmospheric Measurement Techniques, Vol. 10, Iss. 3, 745-758, doi:10.5194/amt-10-745-2017, 2017.

Saunders, R. Hocking, J., Turner, E., Havemann, S., Geer, A., Lupu, C., Vidot, J., Chambon, P., Kopken-Watts, C., Scheck, L., Stiller, O., Stumpf, C. Borbas, E.: RTTOV-13 SCIENCE AND VALIDATION REPORT, pp. 1–106, 2020.

Skofronick-Jackson, G., and et al. : The Global Precipitation Measurement (GPM) mission for science and society. Bull. Amer. Meteor. Soc., 98, 1679–1695, doi: 10.1175/BAMS-D-15-00306.1, 2017.

Todling, R., and El Akkraoui, A.: The GMAO hybrid ensemble-variational atmospheric data assimilation system:Version 2.0. NASA/TM-2018-104606, Vol. 50, 184 pp., 2008.

Wang, D., Prigent, C., Kilic, L., Fox, S., Harlow, C., Jimenez, C., Aires, F., Grassotti, C., Karbou, F.: Surface emissivity at microwaves to millimeter waves over polar regions: Parameterization and evaluation with aircraft experiments, *Journal of Atmospheric and Oceanic Technology*, 34(5), pp. 1039–1059, doi: 10.1175/JTECH-D-16-0188.1, 2017.

Weng, F., Yan, B. and Grody, N. C.: A microwave land emissivity model, Journal of Geophysical Research Atmospheres, 106(D17), pp. 20115–20123, doi: 10.1029/2001JD900019, 2001.

Zhu, Y., Todling, R. and Jin, J.: Improving the use of surface-sensitive radiances in the GMAO GEOS system, The 23rd International TOVS Study Conference, http://cimss.ssec.wisc.edu/itwg/itsc/itsc23/agendas/posters/poster.2p.20.zhu.pdf, 2021

National Aeronautics and
Space Administration

E-mail: bryan.m.karpowicz@nasa.gov | *Web:* gmao.gsfc.nasa.gov